

References

- Bejan, A., 1979, "A Study of Entropy Generation in Fundamental Convective Heat Transfer," *ASME JOURNAL OF HEAT TRANSFER*, Vol. 101, pp. 718-725.
- Bejan, A., 1996, *Entropy Generation Minimization—The Method of Thermodynamic Optimization of Finite-Size Systems and Finite-Time Processes*, CRC Press Inc., New York.
- Evans, R. B., Kadaba, P. V., and Hendrix, W. A., 1983, "Essergetic Functional Analysis for Process Design and Synthesis," *Efficiency and Costing*, ACS Symposium Series, pp. 239-261.
- Fowler, A. J., and Bejan, A., 1994, "Correlation of Optimal Sizes of Bodies with External Forced Convection Heat Transfer," *Int. Comm. Heat Mass Transfer*, Vol. 21, pp. 17-27.
- Guyer, E. C., and Brownell, D. L., 1989, chap. 5, *Handbook of Applied Thermal Design*, McGraw-Hill Book Company, New York.
- Gebhart, B., 1971, *Heat Transfer*, McGraw-Hill Book Company, New York, pp. 212-214, 270.
- London, A. L., and Shah, R. K., 1983, "Costs of Irreversibilities in Heat Exchanger Design," *Heat Transfer Engineering*, Vol. 4, No. 2, pp. 59-73.
- Poulikakos, D., and Bejan, A., 1982, "Fin Geometry for Minimum Entropy Generation in Forced Convection," *ASME JOURNAL OF HEAT TRANSFER*, Vol. 104, pp. 616-623.
- Ranasinghe, J., Aceves-Saborio, S., and Reistad, G. M., 1987, "Optimization of Heat Exchangers in Energy Conversion Systems," *Second Law Analysis of Thermal Systems*, M. J. Moran and E. Sciubba, eds., ASME, New York, pp. 29-38.
- Shuja, S. Z., and Zubair, S. M., 1997, *Thermoeconomic Design and Analysis of Constant Cross-Sectional Area Fins*, KFUPM Mechanical Engineering Department Report, Saudi Arabia.
- Tribus, M., and Evans, R. B., 1962, "A Contribution to the Theory of Thermoeconomics," *UCLA Engng. Dept.*, Report No. 62-36, Los Angeles, CA.
- von Spakovsky, M. R., and Evans, R. B., 1989, "The Design and Performance Optimization of Thermal System Components," *ASME Journal of Energy Resources Technology*, Vol. 111, pp. 231-238.
- Zubair, S. M., Kadaba, P. V., and Evans, R. B., 1987, "Second-Law-Based Thermoeconomic Optimization of Two-Phase Heat Exchangers," *ASME JOURNAL OF HEAT TRANSFER*, Vol. 109, pp. 287-294.

Electromagnetic Heating of Spheres

R. W. Shampine¹ and Y. Bayazitoglu²

Nomenclature

- $\mathbf{A}_n(r, u, \phi)$ = vector potential due to the n th current source
- a_0 = loop radius, m
- C = capacitance, F
- f = frequency of current, Hz
- $H_i(q_n)$ = skin depth function for power absorbed
- $I_{l+1/2}$ = modified Bessel function
- I_0 = peak coil current, A
- $I_{n,l,m}$ = source function for the n th current source, A
- \mathbf{J}_s = current density, A/m²
- $J_{l+1/2}$ = Bessel function of the first kind
- L = inductance, H
- N = number of loops
- P_0 = characteristic power, W
- P_s = power dissipated in the sphere, W
- $P_l^m(\cos \phi)$ = associated Legendre polynomial of the first kind

¹ Assoc. Mem. ASME, Department of Mechanical Engineering and Materials Science, Rice University, 6100 South Main Street, Houston, TX 77005.

² H. S. Cameron Chair Professor of Mechanical Engineering, Fellow ASME, Department of Mechanical Engineering and Materials Science, Rice University, 6100 South Main Street, Houston, TX 77005; bayaz@rice.edu

Contributed by the Heat Transfer Division of THE AMERICAN SOCIETY OF MECHANICAL ENGINEERS. Manuscript received by the Heat Transfer Division December 4, 1996; revision received May 12, 1997; Associate Technical Editor: T. L. Bergman.

- q_n = ratio of the radius to the skin depth = $R_s \sqrt{\pi f \mu_0 \sigma_s}$
- R_s = sphere radius
- $x_{l+1/2,k}$ = k th real root of $J_{l+1/2}(x_{l+1/2,k}) = 0$
- $Y_l^m(u, \phi)$ = spherical harmonic
- $\delta_{l,m}$ = kronecker delta function
- σ_s = sphere electrical conductivity, $(\Omega\text{m})^{-1}$

Introduction

A commonly encountered problem in induction heating and levitation work is the determination of the heat generated in the workpiece or, conversely, the determination of the coil and generator parameters necessary for a specified heat input. In this paper, we describe a series of experiments to verify theoretical predictions of the heating in conducting spheres.

Induction heating and electromagnetic levitation use coils of water-cooled copper tubing that carry large high frequency currents (more than 100 amps, on the order of 500 kHz) surrounding a conducting specimen. The magnetic field generated by this coil induces eddy currents in the specimen, which then dissipate energy in ohmic heating. These currents also interact with the applied field and produce Lorentz forces. However, in this paper, we are only concerned with the heat generated.

Experimental Apparatus

The experimental apparatus was designed to vary the ratio of radius-to-skin depth, q_n , over as wide a range as possible above and below 1 and to measure the heat generated in a metal sphere. The experimental set up, shown schematically in Fig. 1, consisted of a well insulated sphere with a thermocouple in it, surrounded by a water cooled coil. The coil, with a parallel resonant capacitor, was driven by a power amplifier which, in turn, was fed by a stable sine-wave oscillator. Coil current, coil frequency, change in temperature of the sphere, and time were measured during the experiment.

A coil with only a few turns, as is commonly used in induction heating, would have been impractical, as the heating rates we could achieve would have been too low to measure with the available current. More turns imply higher effective currents and thus higher heating, however, this lowers the maximum frequency of operation. A 100-turn coil was chosen with a 12.74 \pm .01 cm inside diameter, a 16.00 cm outside diameter, and a height of 2.02 cm. It had a nearly square cross section and yielded an equivalent single turn radius of 7.18 cm. The coil was water cooled to eliminate an error term due to the coil heating significantly over room temperature, as seen in Shampine et. al. (1996). To increase the current in the coil, parallel resonant capacitors were used. These capacitors carry significant alternating currents and must be carefully chosen to survive this application. Ideally, this combination draws no current when driven at its resonant frequency. In reality, it draws current to make up the losses in the coil, capacitor, and sphere. The resonant frequency f_0 is

$$f_0 = 1/2\pi\sqrt{LC}$$

and can be located by searching for the minimum current drawn

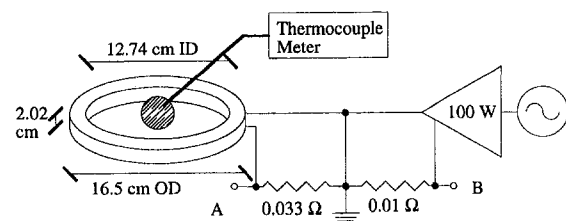


Fig. 1 Experimental apparatus for measuring electromagnetic heating

by the system. At the resonant frequency, most of the current drawn will be at twice the applied frequency (making identification easy on an oscilloscope). For very large capacitors, there will be significant losses in the capacitors and the system will still draw noticeable current at the resonant frequency. Using the resonant circuit, currents in the coil were up to 15.4 times larger than the current supplied by the 100 watt amplifier used to drive the system (due to the energy storage). Coil currents between 14.4 and 22.8 Amps peak were measured using current shunt A. The very low value of this resistor minimized the unavoidable losses in the resonant system. Current shunt B was used to measure the current supplied by the amplifier to prevent overload.

A highly stable RC oscillator was used to provide sine wave drive to the power amplifier. The oscillator drifted less than 0.02 percent over 25 minutes. The period of the sine wave was measured with an eight digit counter, averaging over at least 100 cycles, yielding a frequency accurate to 1 part in 10^8 .

To fully verify the heating trends, we needed to vary q_n both above and below 1. For the low range, a 2.5387 ± 0.0003 cm lead ball with a thermocouple cast into it was used. This allowed us to measure heating for q_n between 0.4 and 1.4. For the range from 1.1 to 4.4, we used machined copper and aluminum balls (2.5154 cm and 2.4928 cm, respectively) with thermocouples swaged into their centers through a drilled hole. To minimize error due to the thermocouple holes, we used 0.0251 cm wire, and oriented the thermocouple exit hole parallel to the axis of the coil. Knowing the masses of the spheres (92.40 ± 0.005 g, 75.33 g, and 23.29 g, respectively), and having measured the heating rate due to an applied magnetic field and assuming perfect insulation, the power input to the spheres is determined.

Measuring the heating rate accurately required that we minimize the heat transfer and measure the temperature. Minimizing heat transfer was done with 2.54 cm of Styrofoam insulation on all sides of the sphere. The thermal time constant of the system was measured to be 1500 s, much longer than the experimental period of 300 s (shorter if the sphere temperature change reached 19.9°C). Thus, for our experiments, the sphere can be assumed to be thermally isolated, and a transient heating analysis was valid.

To achieve reasonable accuracy with heating rates down to 32 mW, we built a thermocouple reader producing 10 millivolts per $^\circ\text{C}$ with an adjustable zero feeding a 3.5 digit meter. The meter was calibrated and yielded $\pm 0.01^\circ\text{C}$ measurements, an order of magnitude more accurate than conventional instruments. The device was sufficiently sensitive that it had to be shielded from air currents to prevent drift. If this was not done, it could have exhibited random drift as much as $\pm 0.15^\circ\text{C}$ in the laboratory environment. The schematic is shown in Fig. 2.

The repeatability of the apparatus was tested by taking multiple experimental runs using a variac to provide a stable 60 Hz wave. These were necessarily less repeatable than data taken with the power amplifier and function generator due to the limited accuracy of setting the variac (± 0.1 amp). The tests were performed with equipment only able to measure current to ± 0.1 amp (four times less accurate than the equipment used in the main experiments), yet still yielded a 95 percent confidence interval of 10.53 ± 0.09 milliwatts (or ± 0.86 percent accuracy), implying that the experimental apparatus produced repeatable results.

Theoretical Predictions

The power dissipated in a sphere in a magnetic field is proportional to the square of the current induced in it and can be expressed, as in the work of Lohofer (1989), as

$$P_s = \frac{1}{2\sigma_s R_s} \sum_{n=1}^N \sum_{l=0}^{\infty} \sum_{m=-l}^l H_l(q_n) \times (|\mathbf{I}_{n,l,m}|^2 + 2 \sum_{n'>n} \delta_{\omega_n, \omega_{n'}} \text{Re}\{\mathbf{I}_{n,l,m} \cdot \mathbf{I}_{n',l,m}^*\}). \quad (1)$$

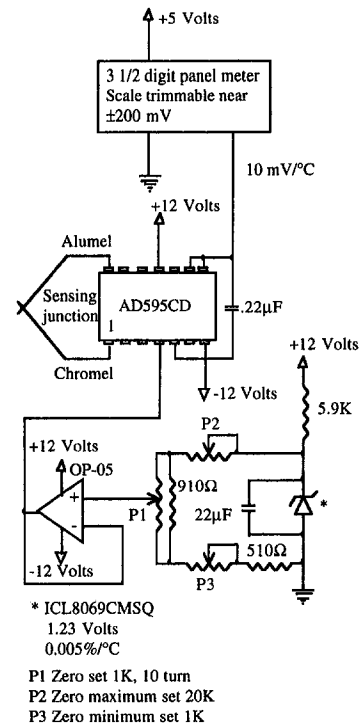


Fig. 2 High resolution thermocouple meter

The first sum, n , is over the loops. The other sums, l and m , are indices of spherical harmonics involved in the solution. For the case where all the loops carry currents of the same frequency (the typical implementation), this can be simplified to

$$P_s = \frac{1}{2\sigma_s R_s} \sum_{l=0}^{\infty} \sum_{m=0}^l H_l(q_n) (2 - \delta_{m,0}) \left| \sum_{n=1}^N \mathbf{I}_{n,l,m} \right|^2.$$

We are interested in the key parameter q_n , and its effect on the dimensionless power $P_s/N^2 P_0$. High frequency currents flow primarily near the surface of conductors, and the skin depth is where the current density has decayed to $1/e$ of its value at the surface. For higher frequency and higher conductivity, this depth decreases. The characteristic power P_0 is a measure of the maximum power that could be dissipated in a sphere of radius a_0 .

$$P_0 = I_0^2 / \sigma_s a_0$$

N is the number of turns in the coil, and I_0 is the peak coil current. The "skin depth" function $H_l(q_n)$ and the vector $\mathbf{I}_{n,l,m}$ are defined in Bayazitoglu and Sathuvalli (1994) as

$$H_l(q_n) = -4q_n^2 \text{Im} \left[\frac{1}{2(1+i)q_n} \frac{I_{l+1/2}\{(1+i)q_n\}}{I_{l-1/2}\{(1+i)q_n\}} \right]$$

$$\mathbf{I}_{n,l,m} = \frac{x_{l+1/2,k}^2}{\mu_0 R_s^{5/2} J_{l+1/2}(x_{l+1/2,k})} \times \int_0^{R_s} \int_{-1}^{+1} \int_0^{2\pi} r^{3/2} J_{l+1/2}(x_{l+1/2,k} r/R_s) \times Y_l^m(u, \phi) \mathbf{A}_n(r, u, \phi) d\phi du dr$$

$$Y_l^m(u, \phi) = (-1)^m \left(\frac{(2l+1)}{4\pi} \right)^{1/2} \frac{(1-m)!}{(1+m)!} P_l^m(u) e^{im\phi}$$

where $Y_l^m(u, \phi)$ are spherical harmonics, and $P_l^m(u)$ are associated Legendre polynomials of the first kind. The function $H_l(q_n)$ represents the effect of the current distribution within the sphere

on the power dissipated, and the vector $\mathbf{I}_{n,l,m}$ is known as the form function of the magnetic field.

For line currents, $\mathbf{I}_{n,l,m}$ may be expressed as in Bayazitoglu and Sathuvalli (1994):

$$\mathbf{I}_{n,l,m} = I_n R_s^l \mathbf{F}_{n,l,m}$$

where $\mathbf{F}_{n,l,m}$ is integrated over the current loop, rather than the sphere volume. It is found by integrating

$$\mathbf{F}_{n,l,m} = \oint (r'_n)^{-(l+1)} Y_l^{m*}(u'_n, \phi'_n) d\mathbf{s}'_n$$

The primed coordinate system is centered on the sphere. If a sphere is positioned at $(x_0, 0, z_0)$ with respect to the center of a current loop of radius a_0 , $\mathbf{F}_{n,l,m}$ can be evaluated using the following variables:

$$\begin{aligned} r' &= \sqrt{a_0^2 + x_0^2 + z_0^2 - 2a_0x_0 \cos \phi} \\ u' &= \cos(\arctan(z_0/\sqrt{a_0^2 + x_0^2 - 2a_0x_0 \cos \phi})) \\ \phi' &= \arctan(a_0 \sin \phi / a_0 \cos \phi - x_0) \\ d\mathbf{s}' &= \hat{\phi} a_0 \cos \phi d\phi \end{aligned}$$

The integration is performed for ϕ from zero to two π with a ϕ directed result.

In the case of a sphere that is small relative to the coil, only the $l = 0, m = 0$, and $l = 1, m = \pm 1$ are important in the power calculations, and the following formulae from Bayazitoglu and Sathuvalli (1994) and Bayazitoglu et. al. (1996) are useful:

$$\begin{aligned} H_0(q_n) &= q \frac{\sinh 2q - \sin 2q}{\cosh 2q + \cos 2q} \\ H_1(q_n) &= q \frac{\sinh 2q + \sin 2q}{\cosh 2q - \cos 2q} - 1 \\ \mathbf{I}_{n,0,0} &= 2\sqrt{\pi}/\mu_0 \mathbf{A}_n(r_0, u_0, \phi_0) \\ \mathbf{I}_{n,1,1} &= \sqrt{3\pi}/2 (i\mathbf{u}_x + \mathbf{u}_y)(BR_s/\mu_0) \\ \mathbf{I}_{n,1,-1} &= -\mathbf{I}_{n,1,1}^* \end{aligned} \quad (2)$$

where $\mathbf{A}_n(r_0, u_0, \phi_0)$ is the vector potential of the applied field at the center of the sphere, and B is the magnitude of the magnetic field at the same point. For a single loop, these can be found in Smythe (1989):

$$\begin{aligned} k^2 &= 4a_0r/[(a_0 + r)^2 + z^2] \\ m &= [1 - (1 - k^2)^{1/2}]/[1 + (1 - k^2)^{1/2}] \\ \mathbf{A}_n &= \frac{\mu I_0}{\pi} \left(\frac{a_0}{mr}\right)^{1/2} [K(m) - E(m)] \\ &= \frac{\mu I_0}{4} \left(\frac{a_0}{r}\right)^{1/2} m^{3/2} \left(1 + \frac{3}{8}m^2 + \frac{15}{64}m^4 + \dots\right) \\ B &= [B_r^2 + B_z^2]^{1/2} \\ B_r &= \frac{\mu I_0}{2\pi} \frac{z}{r[(a+r)^2 + z^2]^{1/2}} \\ &\quad \times \left[-K(m) + \frac{a^2 + r^2 + z^2}{(a-r)^2 + z^2} E(m)\right] \\ B_z &= \frac{\mu I_0}{2\pi} \frac{1}{r[(a+r)^2 + z^2]^{1/2}} \\ &\quad \times \left[K(m) + \frac{a^2 - r^2 - z^2}{(a-r)^2 + z^2} E(m)\right] \end{aligned} \quad (3)$$

K and E are complete elliptic integrals of the first and second kind, respectively. Multiple loops are treated by summing the contributions of each loop. $H_0(q_n)$ and $H_1(q_n)$ can be expressed in the following form in order to develop limiting cases for the power generation:

$$\begin{aligned} \lim_{q_n \rightarrow 0} H_0(q_n) &\approx q_n^4 \\ H_1(q_n) &\approx 0.091 q_n^4 \quad \left. \vphantom{\lim_{q_n \rightarrow 0}} \right\} q_n \leq 1 \\ H_0(q_n) &\approx q_n \\ H_1(q_n) &\approx q_n - 1 \quad \left. \vphantom{\lim_{q_n \rightarrow 0}} \right\} q_n \geq 2 \end{aligned}$$

These imply that the power absorbed by the sphere will vary for where q_n^4 where $q_n < 1$ and for q_n where $q_n > 1$.

Routines were developed to evaluate the small sphere approximation, a single loop exact solution, and a 100 loop exact solution. Using the model for one turn, it was verified that for this system only the $l = 0$ and $l = 1$ modes are important (the $l = 2$ mode makes a 0.3 percent contribution). Comparing the results to the highest q_n experimental value (4.4), we find that the predicted heating decreases with the accuracy of the model.

Small Sphere	$P_s/N^2 P_0 = 0.785$
1 Loop	$P_s/N^2 P_0 = 0.745$
100 Loops	$P_s/N^2 P_0 = 0.702$
Experiment	$P_s/N^2 P_0 = 2.019$

There is a 12 percent difference between the exact theoretical solution and the approximation—implying that the approximation is reasonable. However, at this extreme there is a large difference between any of the theoretical solutions and the measured value.

Experimental Results

Using Eq. (2) for $H_l(q_n)$ and Eq. (3) for $\mathbf{I}_{n,l,m}$ in solving Eq. (1), we developed a fast and simple routine for predicting the heat generation for reasonably sized spheres. Theory predicts that the function $P_s/N^2 P_0$ will vary for q_n^4 where q_n is less than one and for q_n where q_n is greater than one. The experimental values clearly show this behavior and agree well with the predictions up to a q_n of about 2. For the low q_n regime, both the theoretical and experimental results can be fitted to the following q_n^4 curve with correlation coefficients of 0.98745 and 0.99482, respectively.

$$P_s/n^2 P_0 = 0.027898 q_n^4$$

The agreement is not as good for higher q_n . While both the copper and aluminum spheres show the expected linear relationship between q_n and $P_s/N^2 P_0$, they have different slopes and the theory shows a third slope. For q_n greater than 2, the slopes are

Copper	$0.7341 q_n$
Aluminum	$0.9706 q_n$
Theory	$0.2280 q_n$

The correlation coefficients are 0.9846, 0.9755, and 0.9998, respectively.

Comparing the experimental results and theoretical predictions over two orders of magnitude of q_n and five orders of

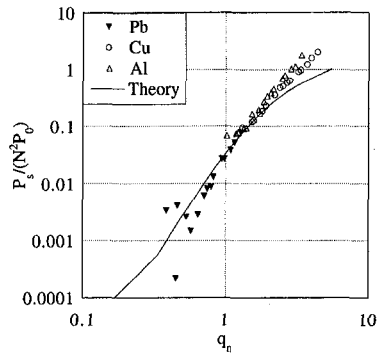


Fig. 3 Experimental and theoretical relationship between normalized power (P_s/N^2P_0) and the ratio of radius to skin depth (q_n) at $x = 0.48$ cm and $z = 0.58$ cm

magnitude of P_s/N^2P_0 (Fig. 3), the agreement is very good, except for high values of q_n . At the low end of the range, the experimental data shows increasing noise due to the very low heating values.

Uncertainty Analysis

The uncertainty analysis is based on linear regression and the method outlined by Bragg (1974). We are interested in the uncertainty in the two dimensionless groups: q_n and P_s/N^2P_0 . The uncertainty in q_n can be expressed as

$$\partial q_n = \left((\pi f \mu_0 \sigma_s)^{1/2} \delta R_s \right)^2 + \left(R_s (\pi \mu_0 \sigma_s / f)^{1/2} \delta f \right)^2 + \left(R_s (\pi \mu_0 \sigma_s / f)^{1/2} \delta \sigma_s \right)^2 \Bigg)^{1/2}$$

where δf is ± 0.01 ppm, δR_s is $\pm 2.54 \times 10^{-6}$, and $\delta \sigma_s$ is ± 0.39 percent; for the range of q_n considered in this work (0.4 to 4.4), this is only 0.02 percent.

For the denominator of the second dimensionless group we find

$$\delta(N^2P_0) = \left((\delta I_0 2N^2 I_0 / \sigma_s a_0)^2 + (-\delta a_0 N^2 I_0^2 / \sigma_s a_0^2)^2 + (-\delta \sigma_s N^2 I_0^2 / \sigma_s^2 a_0^2)^2 \right)^{1/2}$$

While there is no uncertainty in N , and a_0 is known to ± 0.001 m, I_0 is only known to ± 0.03 amps, yielding a worst case N^2P_0 uncertainty of ± 1.4 percent. δP_s is found from

$$\delta P_s = \left((cm\delta\beta)^2 + (\beta c\delta m)^2 \right)^{1/2}$$

β and $\delta\beta$ are found from the experimental data using linear

regression. The 95 percent confidence limit for variance in the heating rate $\delta\beta$ is ± 2.2 percent, and δm is 5×10^{-6} . The 95 percent confidence interval for power is ± 2.2 percent. Finally, the variance in dimensionless power P_s/N^2P_0 is

$$\delta(P_s/N^2P_0) = \left(\frac{(\delta P_s/N^2P_0)^2 + (-\delta(N^2P_0)P_s/(N^2P_0)^2)^2}{(-\delta(N^2P_0)P_s/(N^2P_0)^2)^2} \right)^{1/2}$$

The confidence interval for this is 2.6 percent.

Conclusions

The results of this work clearly indicate that a simplified theoretical model can be used to predict the heat generated in levitated or heated spheres with good accuracy. This has been verified for radius-to-skin depth ratios (q_n) between 0.4 and 4.4, covering the critical transition range where the electromagnetic field just penetrates to the center of the sphere. For q_n below 1, the experimental data agrees well with the theoretical prediction that power dissipated will be proportional to q_n^4 . For q_n above 1, the experimental results provide very reliable data supporting the theoretical prediction that power absorbed is proportional to q_n . Experimental results show excellent quantitative agreement with theoretical predictions up to q_n of about 2 and some difference above this.

Acknowledgments

This work was supported in part by the Texas Advanced Technology Program under grant number 003604-041 and by the National Science Foundation under grant number CTS-9312379. The authors would also like to acknowledge the efforts of Pascal Haas.

References

- Bayazitoglu, Y., and Sathuvalli, U. B., 1994, "Eddy Current Heating in an Electrically Conducting Sphere," *J. of Materials Processing and Manufacturing Science*, Vol. 3, No. 2, pp. 117-141.
- Bayazitoglu, Y., Sathuvalli, U. B., Suryanarayana, P., and Mitchell, G., 1996, "Determination of Surface Tension From the Shape Oscillations of an Electromagnetically Levitated Droplet," *Physics of Fluids*, Vol. 8, No. 2, pp. 370-383.
- Bragg, G. 1974. *Principles of Experimentation and Measurement*, Prentice-Hall, Inc., Englewood Cliffs, New Jersey.
- Lohofer, G. 1989, "Theory of an Electromagnetically Levitated Metal Sphere I: Absorbed Power," *SIAM J. Appl. Math.*, Vol. 49, pp. 567-581.
- Rony, P. B., 1969, "The Electromagnetic Levitation Melting of Metals," *Trans. Vacuum Metallurgy Conference*, American Vacuum Society, Boston, MA., pp. 55-135.
- Shampine, R. W., Sathuvalli, U. B., Bayazitoglu, Y., 1996, "An Experimental Verification of Electromagnetic Heating of Spheres," presented at the ASME National Heat Transfer Conference, August 1996, HTD-Vol. 1, pp. 303-307.
- Smythe, W. R., 1989, *Static and Dynamic Electricity*, Hemisphere Publishing Co., New York.